We are IntechOpen,
the world's leading publisher of
Open Access books
Built by scientists, for scientists

6,900
Open access books available

185,000
International authors and editors

200M
Downloads

Our authors are among the

154
Countries delivered to

TOP 1%
most cited scientists

12.2%
Contributors from top 500 universities

CLARIVATE ANALYTICS
BOOK
CITATION
INDEX
INDEXED

WEB OF SCIENCE™

Selection of our books indexed in the Book Citation Index
in Web of Science™ Core Collection (BKCI)

Interested in publishing with us?
Contact book.department@intechopen.com

Numbers displayed above are based on latest data collected.
For more information visit www.intechopen.com

Detection of VUV Light with Avalanche Photodiodes

Cristina M. B. Monteiro, Luís M. P. Fernandes
and Joaquim M. F. dos Santos
Instrumentation Centre (CI), Physics Department, University of Coimbra
Portugal

1. Introduction

Silicon avalanche photodiodes are alternative devices to photomultiplier tubes in photon detection applications, presenting advantages that include compact structure, capability to sustain high pressure, low power consumption, wide dynamic range and high quantum efficiency, covering a wider spectral range. Therefore, they provide a more efficient conversion of the scintillation light into charge carriers. Major drawbacks are lower gains, of few hundreds, higher detection limits and non-uniformities in the percent range.

Windowless APDs with spectral sensitivity extended downto the VUV region (~120 nm) have been developed by API [1], RMD [2] and Hamamatsu [3]. They have been used as photosensors for scintillation light produced in noble gases [4-6] and liquids [7-10] for X- and γ-ray spectroscopy applications. Up to now, the main application of APDs as VUV detectors is aimed for a neutrinoless double beta decay experiment using high pressure xenon [6].

Wide band-gap semiconductor photodiodes such as GaN and SiC are also alternative to photomultiplier tubes in UV detection. However, compared to Si-APDs, they present smaller active area of the order of the mm², with higher wafer non-uniformities, lower quantum efficiency and reduced spectral sensitivity in the VUV region (usually useful above 200 nm). On the other hand, they present some advantages, namely the lower biasing voltages, higher gains with lower leak currents, the solar blind capability. Recent reviews on these APDs can be found in [11-17] and references therein.

Through the last decade, we have investigated the response characteristics of a large area APD from API to the scintillation VUV light produced in gaseous argon and xenon at room temperature [4,5]. The emission spectra for argon and xenon electroluminescence is a narrow continuum peaking at about 128 and 172 nm, respectively, with 10 nm FWHM for both cases [18], and corresponds to the lower limit of the APD spectral response. For the 128 and 172 nm VUV light from argon and xenon scintillation, the effective quantum efficiency, here defined as the average number of free electrons produced in the APD per incident VUV photon is 0.5 and 1.1, respectively, corresponding to a spectral sensitivity of about 50 and 150 mA/W [4,19].

In this chapter, we review and summarize the results of our investigation, namely the gain non-linearity between the detection of X-rays and VUV light [20], the gain dependence on

temperature [21,22], the behaviour under intense magnetic fields [23], the minimum detection limit, i.e. the minimum number of photons detectable above the noise level, and the statistical fluctuations in VUV photon detection [24].

2. APD operation principle

Figure 1 shows the structure of an APD, as well as the electric field profile inside its volume. When a high voltage is applied across the APD, only a small region of the p-layer, near the photodiode surface, remains undepleted - the drift region (1). This region has a residual electric field of some tens of V/cm [19]. In the depleted p-region (2), the electric field increases with depth until a maximum is reached, around 10^5 V/cm [19], near the p-n junction and decreases in the depleted n-region. VUV photons are absorbed in (1) and converted into electron-hole pairs. The resulting primary electrons are driven to the p-n junction by the electric field. Around the junction, they obtain a sufficient amount of energy to produce new electron-hole pairs by impact ionisation, leading to an avalanche process in the multiplication region (3). Charge gains of a few hundred are typical. Gain increases exponentially with the applied voltage, resulting in a significant improvement of the signal-to-noise ratio. Detailed operation principles of the APD have been presented in the literature [25-28].
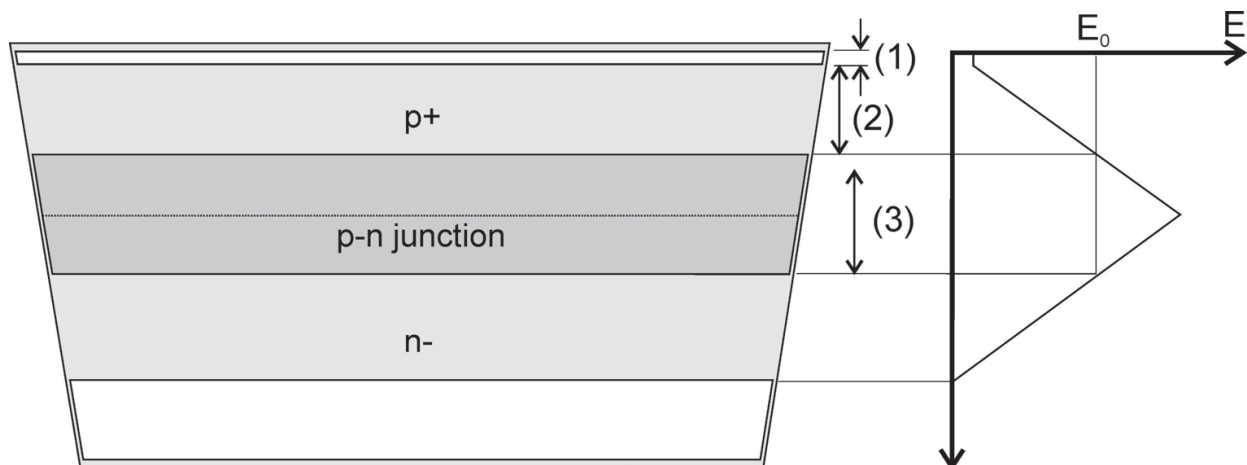

Fig. 1. Schematic of an avalanche photodiode and electric field (E) profile inside its volume. The active region of the APD can be divided in three different parts: the drift region (1), the depleted p-region (2) and the multiplication region (3), where the electric field is higher than the ionisation threshold by electron impact, E_0.

When a voltage is applied to a photodiode in order to bias the p-n junction, a low-intensity current, typically a fraction of µA, is observed. This dark current has its origin in the detector volume and surface. The volumetric dark current results from the continuous generation of charge carriers - minority carriers - on both sides of the junction, which are conducted through that junction, and from the thermal generation of electron-hole pairs in the depletion region, which increases with volume and decreases by cooling. The surface dark current is generated in the p-n junction edges due to high voltage gradients in its vicinity. Since dark current is a noise source and increases considerably with temperature, the electronic noise level can be reduced by cooling the APD, reducing the statistical fluctuations and the minimum detection limit of VUV photons [21,22].

Different studies have proven the APD response characteristics for VUV light to be different from those for visible light, which has been originally used to determine most of the characteristics of photodiodes [20-23]. This is due to the difference in the average interaction depth of the photons, which is approximately 1 μm for 520-nm photons and approximately 5 nm for 172-nm photons [29]. VUV photons interact mainly within the first atomic layers of the wafer, where the electric field is weaker. This results in higher diffusion of the charge carriers, which can be lost to the surface boundary and to impurities.

3. APD noise and statistical fluctuations

The energy resolution associated to radiation detection in avalanche photodiodes is determined by several factors, namely statistical fluctuations associated to the number of electron-hole pairs produced in silicon and the avalanche process (N); gain non-uniformity in the APD detection volume; detector noise, resulting from dark current, and electronic system noise. The total broadening in the energy distributions of APD pulses, ΔE, is the quadratic addition of those three contributions.

The output signal variance, in number of primary electrons, associated to the statistical fluctuations is given by [30]:

$$\sigma_N^2 = \sigma_n{}^2 + N\,(F-1) \tag{1}$$

N being the number of primary electrons, $\sigma_n{}^2$ its variance and F the excess noise factor. F is related to the variance of the electron avalanche gain, $\sigma_A{}^2$, according to:

$$F = 1 + \sigma_A{}^2 / G^2 \tag{2}$$

Due to the discrete nature of the multiplication process, as a result of electron avalanche fluctuations F is higher than 1 and varies with gain, G.

The relationship between F and G has been derived from the McIntyre model considering that photoelectrons are injected close to the p-zone surface [31]:

$$F \cong G\,k_{ef} + \left(2 - \frac{1}{G}\right)\left(1 - k_{ef}\right) \tag{3}$$

k_{ef} being the effective ratio between the ionisation coefficients for holes and electrons. For lower gains, $k_{ef} \ll 1$ and $F \cong 2 - 1/G$.

For the useful gain range (G > 30), the variation of k_{ef} with voltage is very low and considering k_{ef} constant is a good assumption. As a result, the dependence of F on G should be approximately linear, e.g. see [32].

There is a clear difference between light and X-ray detection. In particular, the non-uniformity contribution is negligible in light detection if the whole APD area is irradiated, since the final pulse results from the average response to the entire number of photons interacting in the silicon.

For light pulse detection, the variance of the number of primary electrons is described by Poisson statistics, $\sigma_n{}^2 = N$. The statistical error, in number of primary electrons is, then:

$$\sigma_N{}^2 = N\,F \tag{4}$$

The noise contribution to the energy resolution results from two different sources, namely the detector dark current and the electronic system. Dark current presents two different components. One of them (IDS) does not depend on gain and corresponds to the surface current and to a small fraction of the volumetric current resulting from thermal generation of electron-hole pairs in the n-region, thus non-amplified. The other component (IDV) is amplified by the gain and corresponds to the volumetric current resulting from the production of electron-hole pairs in the p-region. The total current at the APD output is:

$$I = I_{DS} + G\,I_{DV} + G\,I_0 \tag{5}$$

where G is the APD gain and I_0 the non-amplified signal current, corresponding to electron-hole pairs produced by the absorbed radiation.

The noise associated to the electronic system is mainly originated in the FET (field effect transistor) at the preamplifier input. Fluctuations in the FET channel current are similar to the thermal noise and can be represented by a noise equivalent resistance (R_{eq}) in series with the preamplifier input [33].

A detailed noise analysis in avalanche photodiodes has been already presented in the literature [34,35]. If the preamplifier is connected to a linear amplifier with equal differentiation and integration constants, τ, the electronic noise contribution to the peak broadening in units of energy is:

$$\Delta E_N{}^2 = \left(2.36\frac{e\varepsilon}{qG}\right)^2 \left[\frac{k_B\,T\,R_{eq}}{2\tau}C_T{}^2 + \frac{\tau q}{4}\left(I_{DS} + I_{DV}\,G^2\,F\right)\right] \tag{6}$$

q being the electron charge, $e \cong 2.718$ the number of Nepper, k_B the Boltzmann constant (1.38×10^{-23} J/K) and T the temperature (in Kelvin); C_T is the total capacitance at the preamplifier input, including detector and FET input capacitances.

The first term in (6) describes the electronic system noise associated to the detector and the second term corresponds to the dark current contribution. Both terms depend on the shaping time constants used in the linear amplifier. The noise contribution also depends on the gain and the excess noise factor.

4. VUV-light measurements

A Gas Proportional Scintillation Counter (GPSC) was used to provide VUV-light pulses, with a known number of photons, to the APD. The operation principle of the GPSC is described in detail in [36] and a schematic of the counter is depicted in Fig.2. X-rays interact in the absorption region producing a known number of primary electrons. The primary electron clouds are driven to the scintillation region where the electric field is kept below or around the gas ionisation threshold. Therefore, upon traversing the scintillation region, the primary electrons gain enough energy from the electric field to excite a large number of noble gas atoms, leading to a VUV-light pulse as a result of the de-excitation processes of the atoms. Following the incidence of VUV photons on the APD, charge multiplication takes place within the APD volume, originating the final charge pulse at its output. The operational characteristics of the GPSC with APD are described in [4] and [5] for xenon and argon fill gas, respectively.
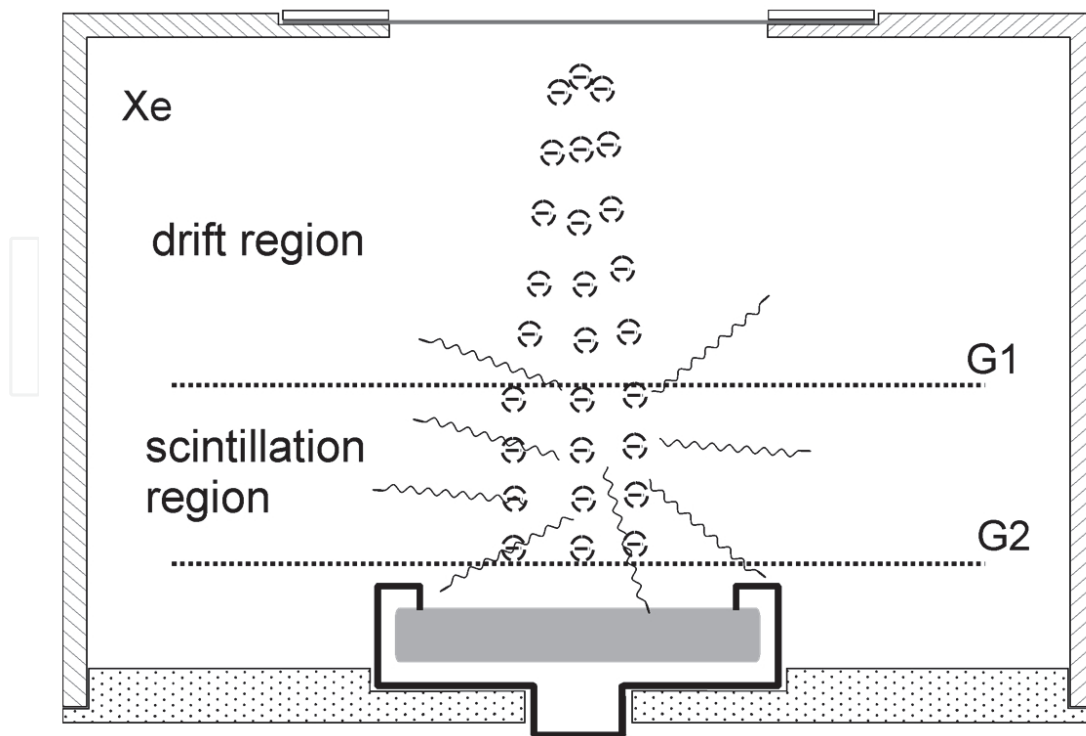
Fig. 2. Schematic of the Gas Proportional Scintillation Counter instrumented with an APD as the VUV photosensor.

The geometry of the GPSC was chosen to allow some of the X-ray photons to reach the APD without being absorbed in the gas, which allows direct X-ray interactions in the APD concomitant with X-ray interactions in the gas. A typical pulse-height distribution is presented in Fig.3 for a GPSC with argon filling, irradiated with 5.9-keV X-rays. The main features of the pulse-height distributions include the scintillation peaks resulting from the full absorption of X-rays in the gas and from events with subsequent argon fluorescence escape from the active volume, the so-called escape peaks, as well as the electronic noise tail. An additional peak resulting from direct absorption of the 5.9-keV X-rays in the APD is also present in the pulse-height distributions. This latter peak is easy to identify, since its amplitude depends only on the APD biasing and not on the GPSC biasing, being present even when the gas proportional scintillation counter biasing is switched off.

Knowing the w-value - i.e. the average energy to produce an electron/hole pair - of silicon for X-rays (w_{Si} = 3.6 eV), the peak resulting from the direct interaction of 5.9-keV X-rays in the APD can be used to determine the number of charge carriers produced by the VUV-light pulse. In the case of Fig.3, the amount of energy deposited in silicon by the argon scintillation pulse is similar to what would be deposited by 30-keV X-rays directly absorbed in the APD. This feature allowed the absolute determination of the argon and the xenon scintillation yields, given the quantum efficiency of the APD and the solid angle subtended by the APD relative to the region where the scintillation occurred [37-40].

The performance characteristics of the APD in VUV light detection has been investigated as a function of voltage applied to the APD, using the information of the successive pulse-height distributions obtained for each voltage. The relative positions of the VUV-light and the direct X-ray interaction peaks provide the information on the non-linear response of the APD to X-rays, important issue for the correct determination of the number of scintillation

photons detected by the APD. Knowing the number of photons hitting the photodiode, the minimum number of photons above the noise that can be detected by the APD can be determined by the relative position of the noise tail. The width of the scintillation peak can be used to determine the statistical fluctuations resulting from the detection and signal amplification processes in the APD, provided that the statistical fluctuations associated with the X-ray interaction in the gas, i.e. in the number of primary electrons produced, and with the gas scintillation processes are known.
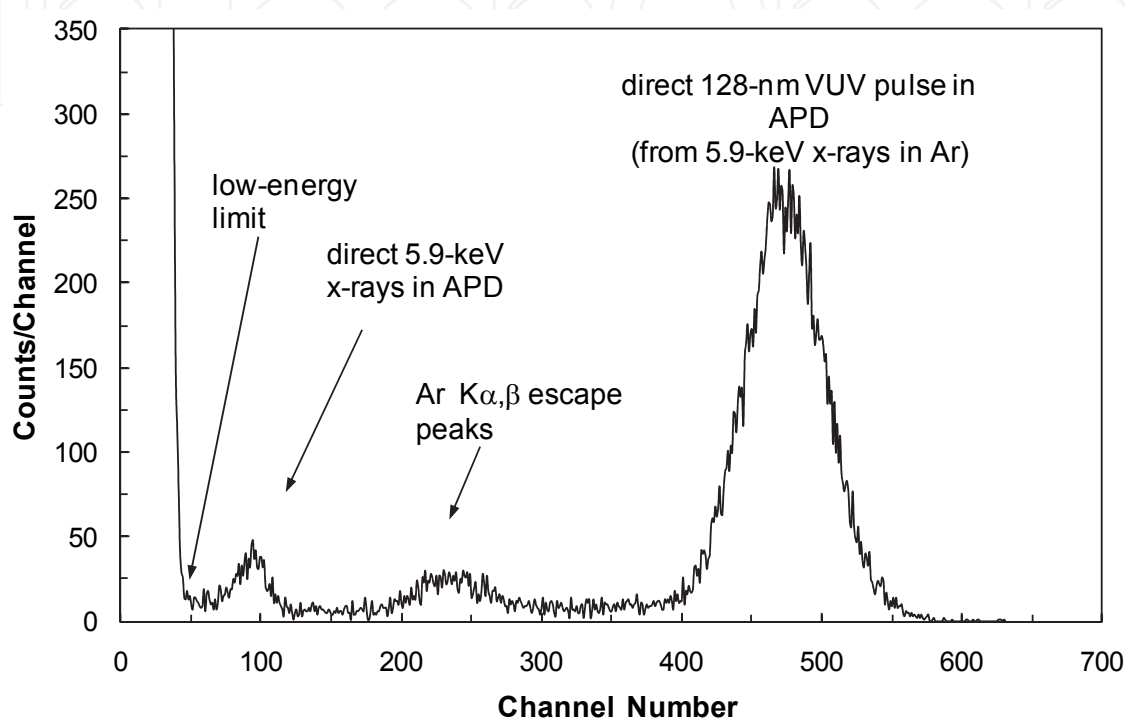
Fig. 3. Typical pulse-height distribution in APDs, resulting from both direct absorption of 5.9-keV X-rays in the APD and 128-nm scintillation absorption in the APD, resulting from the interaction 5.9-keV X-rays in argon.

The APD gain was obtained by normalizing the scintillation pulse amplitude to the manufacturer specification – a gain of 13.8 at 1577 V. The APD gain was also determined for the direct interaction of 5.9-keV X-rays. Typical APD gain variation with voltage applied to the photodiode is presented in Fig.4 for both 5.9-keV X-rays and 128-nm scintillation pulse interactions in the APD.

Figure 4 demonstrates the non-linear effects that are present in X-ray detection. While for light detection the VUV-photon interactions and, consequently, the charge carriers and subsequent electron avalanche are distributed through the whole APD, the point-like nature of the X-ray interaction results in the production of a charge carrier cloud and subsequent electron avalanche that is concentrated in a very small volume of the APD. Therefore, non-linear effects in X-ray detection are attributed to space-charge effects, reducing the local electric field, and to heating in the avalanche region [20,30]. This is confirmed by the non-linearity observed in the APD gain response between X-rays of different energies. When using higher energy X-rays, significantly higher gain reductions were measured, e.g. [41]. In addition, non-linear effects increase with increasing avalanche gain, i.e. with increasing voltage applied to the APD.
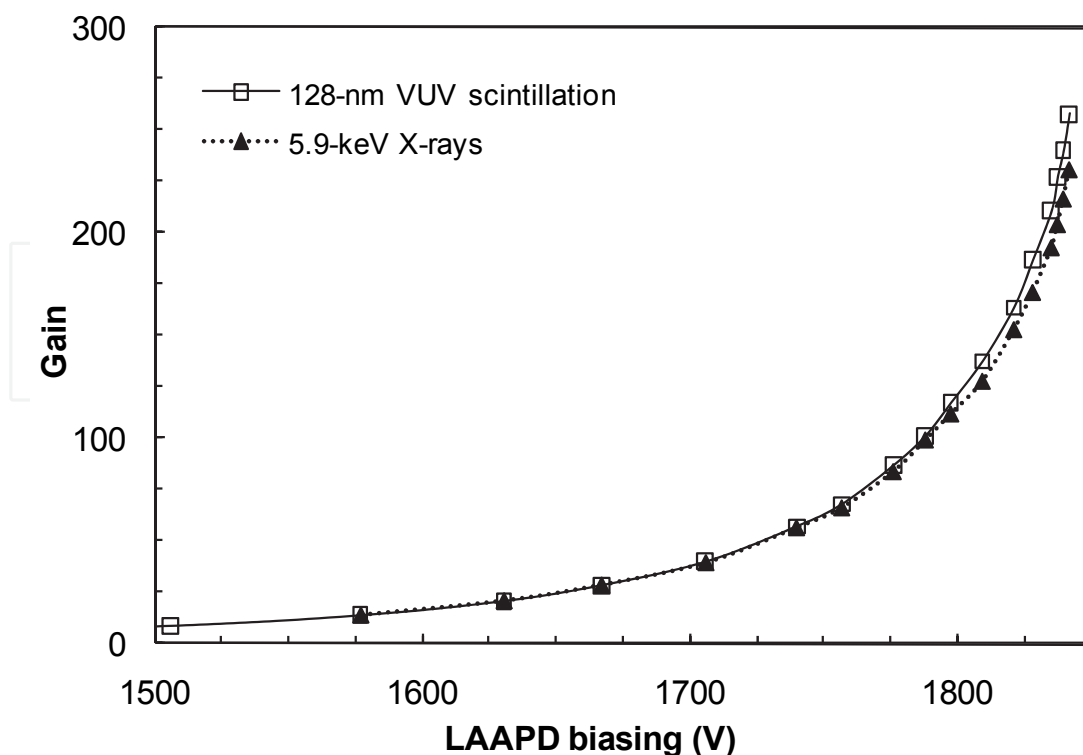
Fig. 4. APD gain for both direct 5.9-keV X-ray absorption in the APD and 128-nm scintillation absorption in the APD as a function of the APD biasing voltage.

5. APD characteristics for xenon scintillation detection (~172 nm)

For the present measurements the number of xenon VUV photons that irradiate the APD is about 2.4×10^4 photons per light pulse.

As mentioned above, significant non-linearity in APD gain response between X-rays and visible light was observed in different types of APDs, being the APDs from API those which present the lowest effects [28], reaching a reduction of 3% in X-ray gain response when compared to visible light. In Fig.5 we present the X-ray-to-xenon-scintillation amplitude ratio as a function of APD biasing. Non-linear effects are less than 3.5% and 7% for gains below 100 and 200, respectively, when considering 5.9-keV X-rays. These non-linearities are higher than those observed for visible-light detection [28,30] but are, nevertheless, smaller than those observed with other types of APDs.

Figure 6 presents the Minimum number of Detectable Photons (MDP) for xenon electroluminescence, defined as the number of photons that would deposit, in the APD, an amount of energy equivalent to the onset of the electronic noise tail. The MDP is approximately constant being, for the present conditions, about 600 photons for 172-nm VUV-light pulses and for gain values above 40, increasing significantly as the gain drops below that value and the signal approaches the noise level.

The obtained MDP can decrease if further efforts are made towards the reduction of the noise level achieved in the present setup. Nevertheless, the MDP can be reduced up to a factor of two by cooling the temperature of the photodiode to values below 0 °C, see section 7.

The results obtained with this APD for MDP at 172 nm are lower than those obtained with the peltier-cooled APD in [21] (~10^3 photons). The difference may be attributed to the differences in the APD dark currents, which limit the electronic noise and, thus, the MDP. It

can also be attributed to the noise level present in both setups. Since the peltier-cooled APD has a different enclosure, with more wiring, it is more prone to electronic noise.
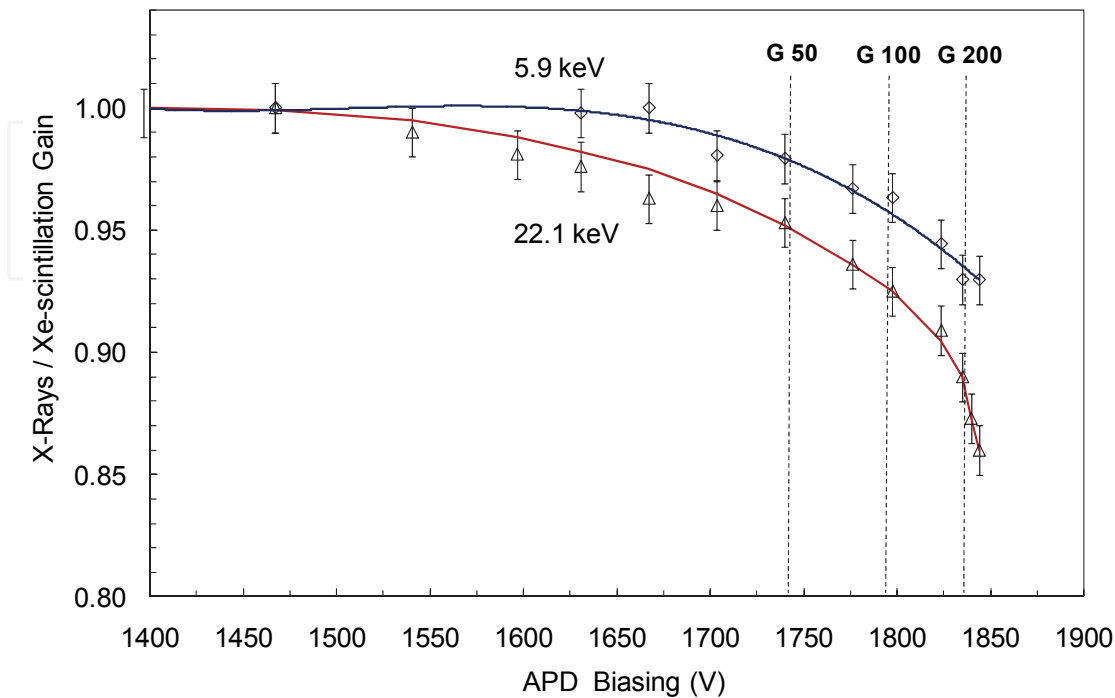

Fig. 5. X-ray to 172-nm scintillation pulse amplitude ratio as a function of APD biasing voltage, for 5.9- and 22.1-keV X-rays.
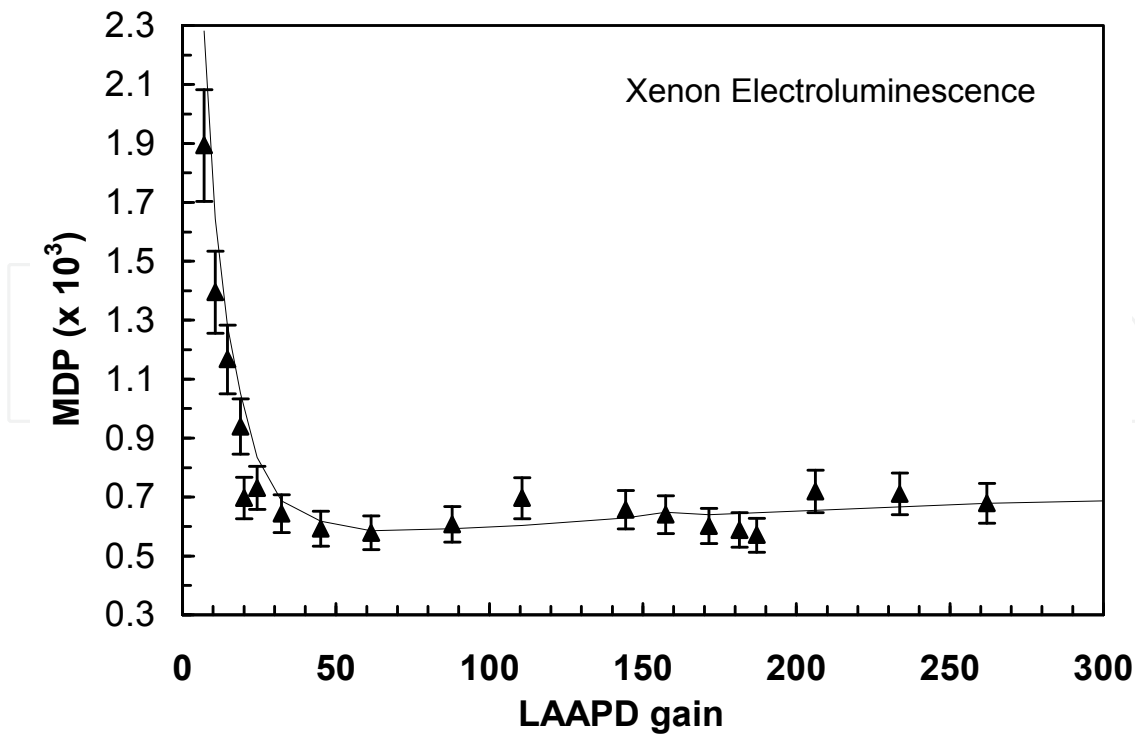

Fig. 6. Minimum number of detectable 172-nm VUV-photons as a function of APD gain. The line serves only to guide the eyes.
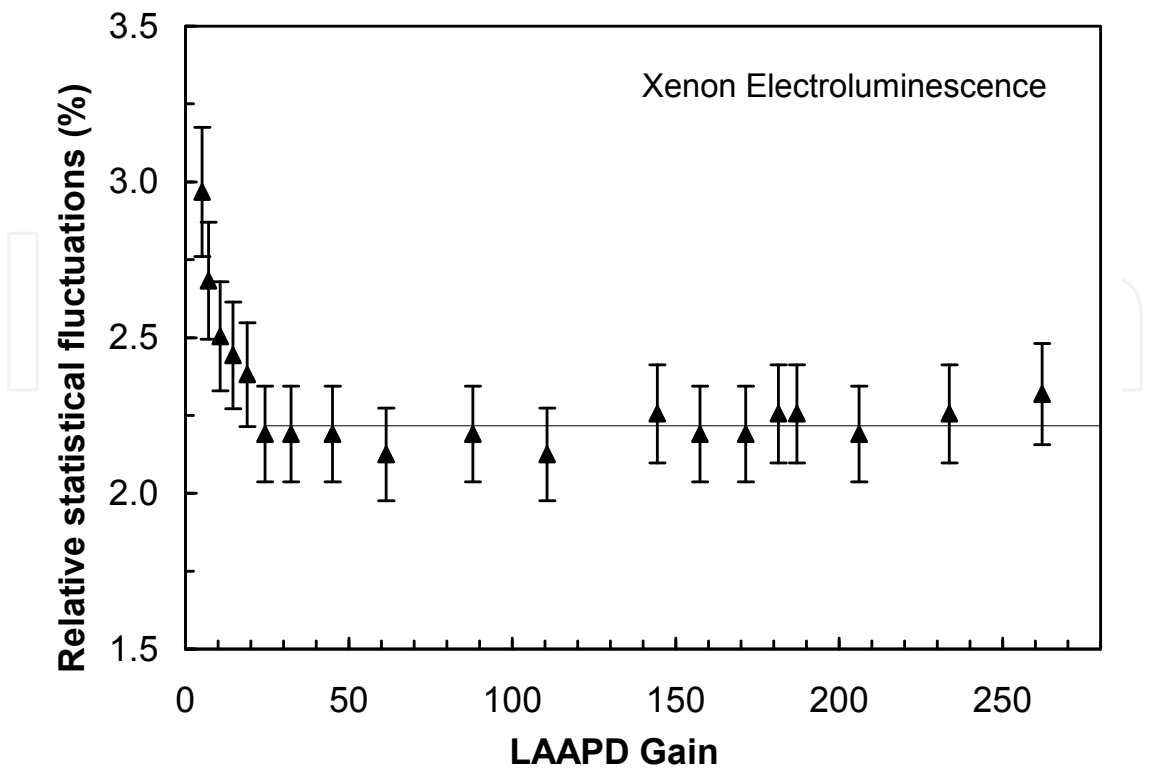
Fig. 7. Relative statistical fluctuations associated to the VUV detection of 2.4×10^4 photons of ~172 nm VUV-light pulses as a function of APD gain. The line serves only to guide the eyes.

The statistical fluctuations associated to the detection of VUV-light in the APD may be estimated from the energy resolution of the pulse-height distributions of 5.9-keV X-ray full absorption in the gas. The energy resolution of a conventional GPSC is determined by the statistical fluctuations occurring in the primary ionisation processes in the gas, in the production of the VUV scintillation photons and in the photosensor. Since the statistical fluctuations associated to the scintillation processes are negligible when compared to those associated to the primary electron cloud formation in the gas and to those associated to the scintillation detection in the photosensor, the energy resolution, R, of the GPSC, for an X-ray energy E_x, is given by [36]

$$R = 2.355\sqrt{\frac{F}{N_e} + \left(\frac{\Delta E}{E}\right)^2} = 2.355\sqrt{\frac{Fw}{E_x} + \left(\frac{\Delta E}{E}\right)^2} \qquad (7)$$

where N_e is the average number of primary electrons produced in the gas by the X-rays, F is the Fano factor, w is the average energy to create a primary electron in the gas and E is the energy deposited by the VUV-radiation in the photosensor.

The statistical fluctuations associated to the VUV-photon detection can be, thus, obtained by

$$\frac{\Delta N_{UV}}{N_{UV}} = \frac{\Delta E}{E} = \sqrt{\left(\frac{R}{2.355}\right)^2 - \frac{Fw}{E_x}} \qquad (8)$$

In the present case, E_x = 5.9-keV, w = 22.4 eV and F = 0.17 for xenon. The relative statistical fluctuations associated to the detection of 2.4×10^4 VUV photons for ~172 nm VUV-light

pulses, as a function of gain, are depicted in Fig.7. The APD relative uncertainty decreases rapidly with the onset of gain, stabilizing for gains above approximately 30 and reaching values of 2.2%. This value can be reduced by cooling the photodiode operating temperature to values around 0 ºC [22].

Figures 6 and 7 show that, for the detection of the light-levels of 172-nm photons presented in this study, best performance characteristics are achieved for gains around 40. However, gains as low as 20 are sufficient to achieve a nearly optimum performance, i.e. without presenting significant degradation of MDP and energy resolution. For lower light levels, higher gains may be needed to pull the signal of the light-pulse out of the noise and achieve the best possible performance.

6. APD characteristics for Argon scintillation detection (~128 nm)

For the present measurements the number of xenon VUV photons that irradiate the APD is about 1.4×10^4 photons per light pulse. As can be seen from Fig.4, the argon scintillation pulse deposits in the APD an amount of energy similar to what would be deposited by the interaction of ~30-keV X-rays in the photodiode.

In Fig.8 we present the X-ray-to-argon-scintillation amplitude ratio as a function of APD biasing. The non-linearity is higher than that found for xenon scintillation, being about 4.5% and 10% for gains about 100 and 200, respectively, when considering 5.9-keV X-rays.
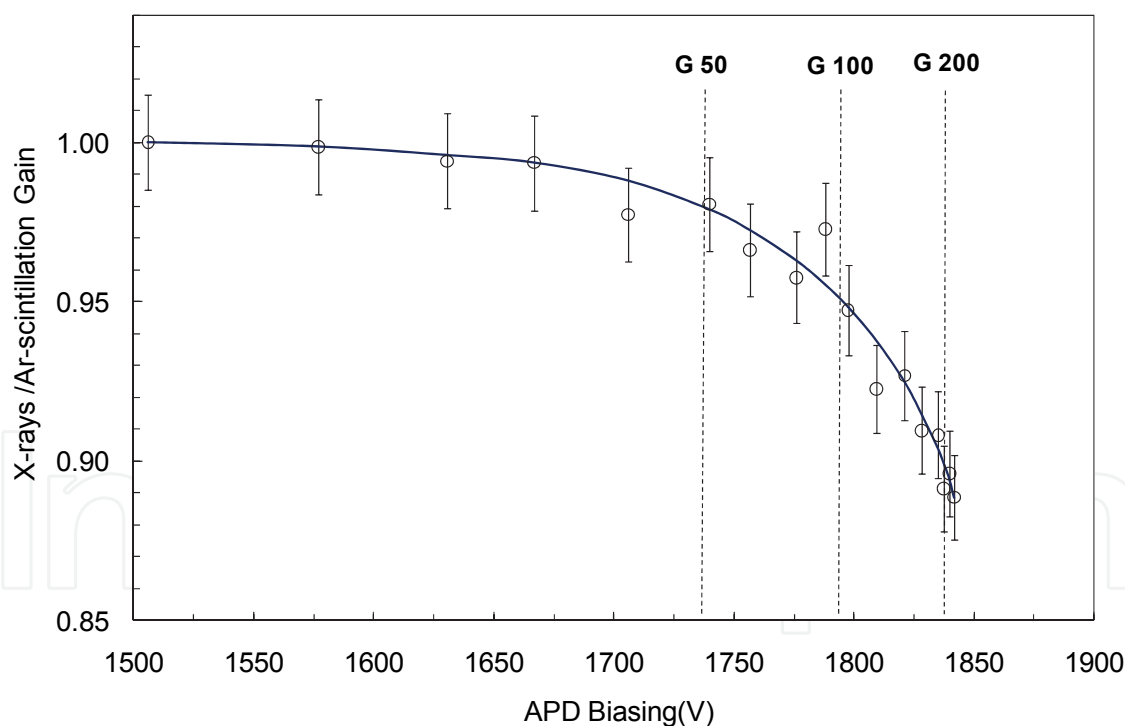

Fig. 8. X-ray to 128 nm pulse amplitude ratio as a function of APD biasing voltage, for 5.9-keV X-rays.

Figure 9 presents the minimum number of detectable photons (MDP) for argon electroluminescence, as defined for the xenon case. The MDP shows a similar trend as for xenon; it is approximately constant, being about 1300 photons for 128-nm VUV-light pulses for gains above 60, increasing significantly as the gain drops below this value.

As for the xenon case, the obtained MDP can decrease if further efforts are made to reduce the noise level of the present setup and can be reduced down to a factor of two by cooling the photodiode to temperatures below 0 °C, see section 7.

As for xenon, the statistical fluctuations associated to the detection of VUV light in the APD may be estimated from the measured energy resolution of the pulse-height distributions of 5.9-keV full absorption in the gas. The statistical fluctuations associated to the VUV-photon detection can, thus, be obtained from (8) where, for argon, w = 26.4 eV and F = 0.30. The relative statistical fluctuations associated to the VUV detection of 1.4×10^4 photons of ~128 nm photons VUV-light pulses, as a function of gain, are depicted in Fig.10. The APD relative uncertainty decreases rapidly with the onset of gain, stabilizing for gains above ~30 and reaching values of 3.9%.

Figures 9 and 10 show that, for the detection of the light-levels of 128-nm photons presented in this study, best performance characteristics are achieved for gains above 60. For gains lower than 60, the MDP increases significantly, while the statistical fluctuations remain constant down-to gains of 20.
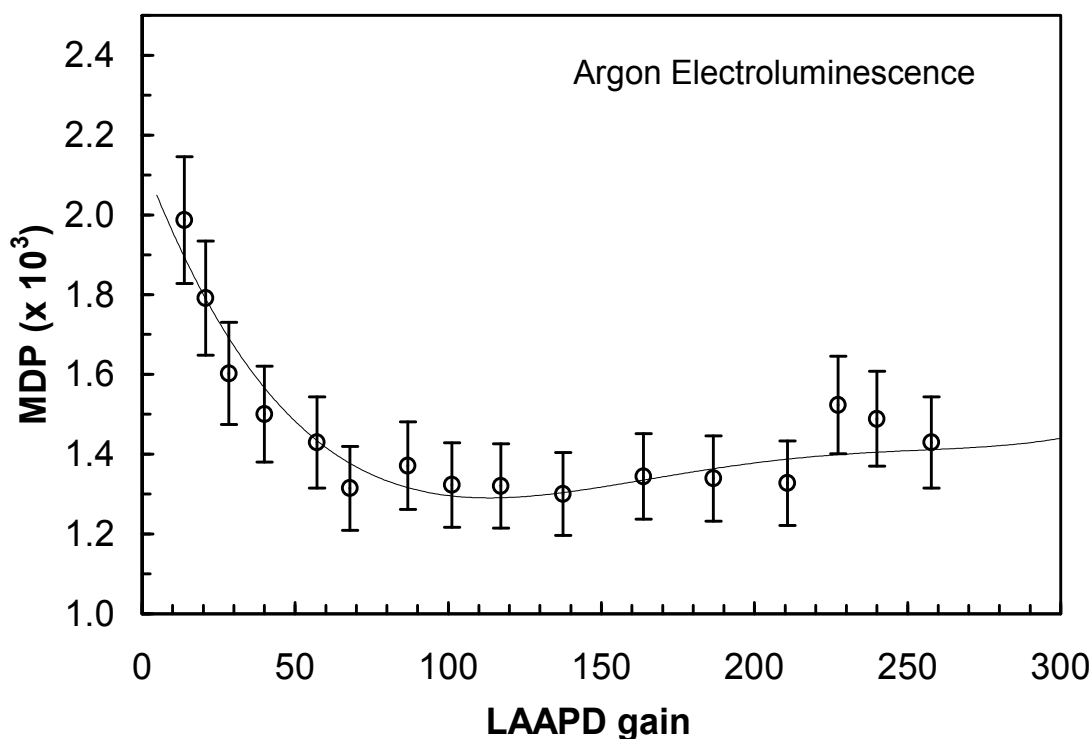
Fig. 9. Minimum number of detectable 128-nm VUV-photons as a function of APD gain. The line serves only to guide the eyes.

7. Temperature dependence

The APD response depends significantly on the operation temperature [22], in particular the gain and the dark current are two parameters that reflect significant dependence on temperature. Therefore, temperature control and stabilization during the measurements may be required, which is a drawback in many applications. In alternative, the knowledge of the gain variation with temperature may lead to corrections that take into account temperature variations during measurements.
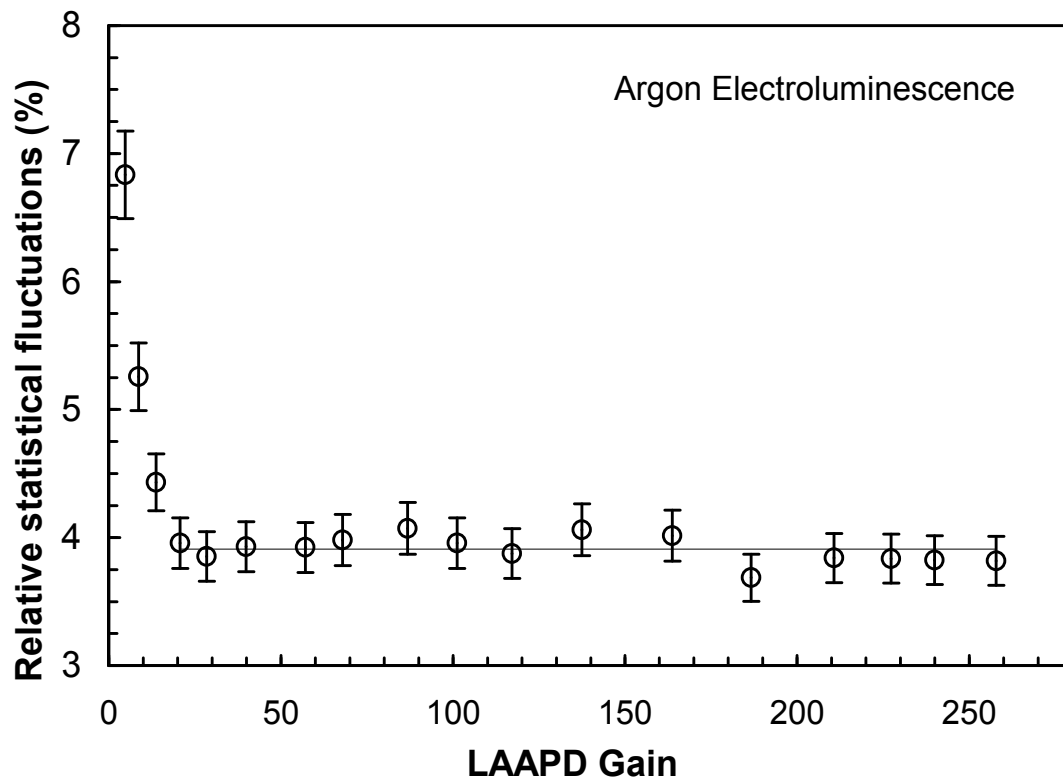
Fig. 10. Relative statistical fluctuations associated to VUV detection of 1.4×10^4 photons of ~128-nm VUV-light pulses as a function of APD gain. The line serves only to guide the eyes.

We have investigated the effect of temperature on gain, dark current, minimum number of detectable photons and statistical fluctuations using an APD with an integrated peltier cell capable of providing minimum operation temperatures of -5°C [21]. Figure 11 depicts the APD gain for VUV photons from xenon and for different operation temperatures. As expected, the gain increases with reducing temperature due to the increase of the silicon resistivity. The maximum gain increases from 300 to 700 as the temperature decreases from 25 to -5°C, respectively.

We can organize the data of Fig.11 and depict the gain as a function of temperature, for different biasing voltages, Fig.12. The gain decreases exponentially with increasing temperature. For each voltage, the relative gain variation is almost constant and increases from -2.7% to -5.6% per °C as the voltage increases from 1633 to 1826 V. The relative gain variation for high biasing voltages is almost a factor of 2 higher than the 3% reported by the manufacturer for visible light detection [19].

The increase in resistivity of the silicon wafer with decreasing temperature has impact on the APD dark current and, therefore, on the electronic noise. Figure 13 depicts the dark current as a function of gain for different operation temperatures. The dark current is reduced by about one order of magnitude as the temperature decreases from 25°C to -5°C. This reduction has a positive impact on the minimum number of detectable photons and on the statistical fluctuations in the APD, as shown in Figs. 14 and 15. The minimum detectable number of photons is reduced from 1300 to 500 as the temperature decreases from 25°C to -5°C.
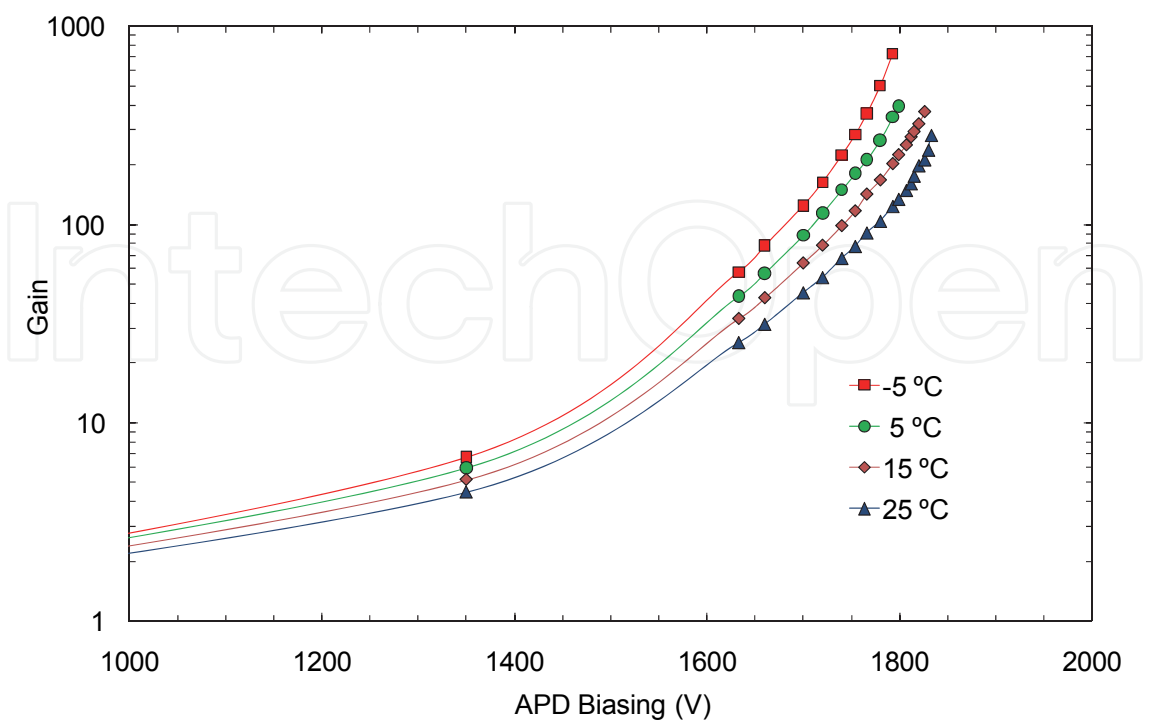
Fig. 11. APD gain for VUV scintillation as a function of APD biasing for different operation temperatures.
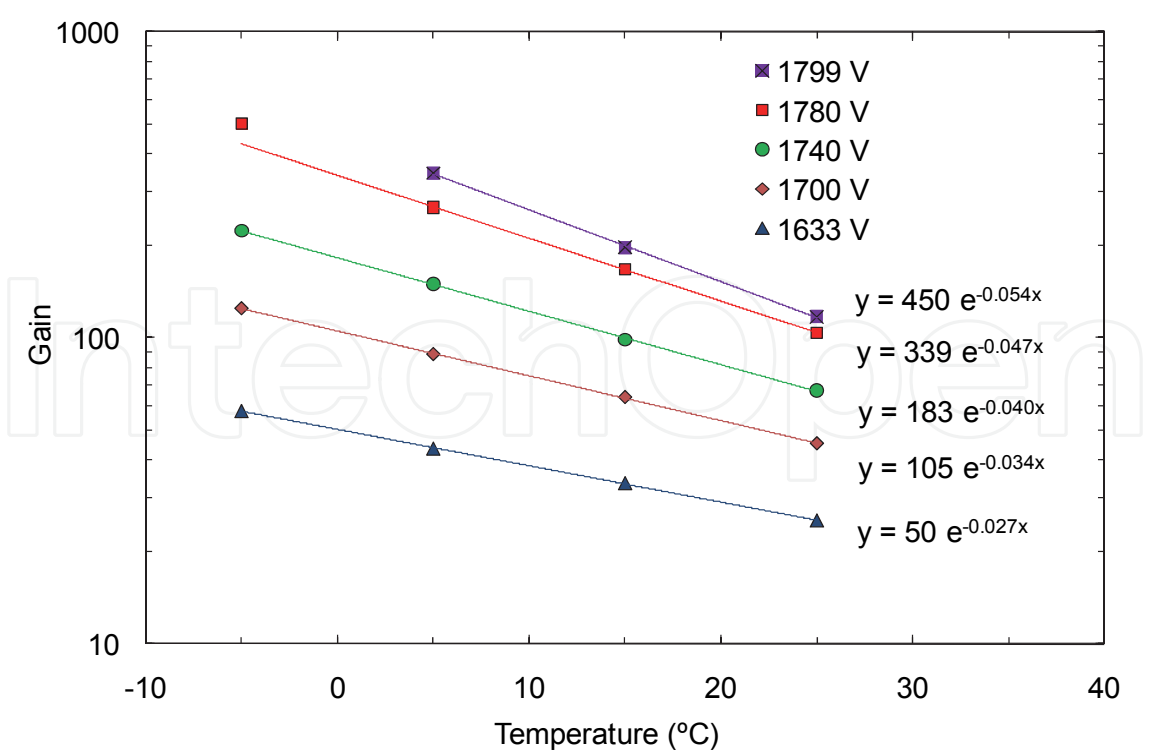

Fig. 12. APD gain for VUV scintillation as a function of APD temperature for different bias voltages.
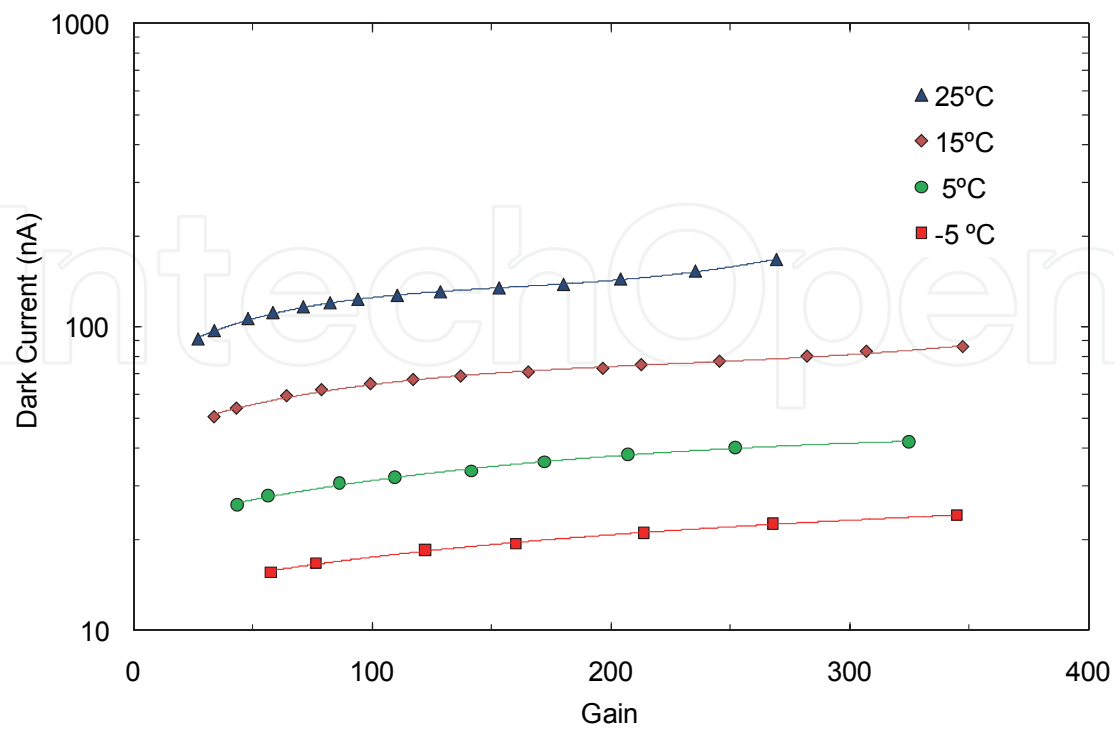
Fig. 13. APD dark current as a function of its gain for different operation temperatures.
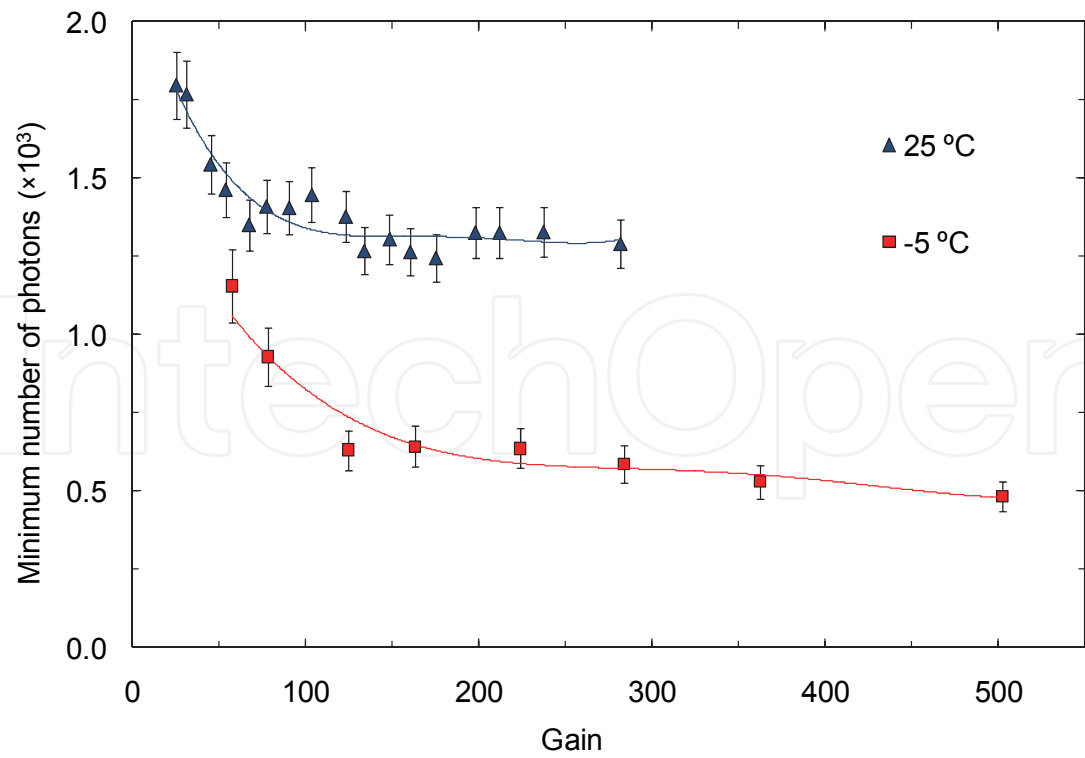
Fig. 14. Minimum number of detectable 172-nm VUV-photons as a function of APD gain for operation temperatures of 25ºC and -5ºC. The lines serve only to guide the eyes.
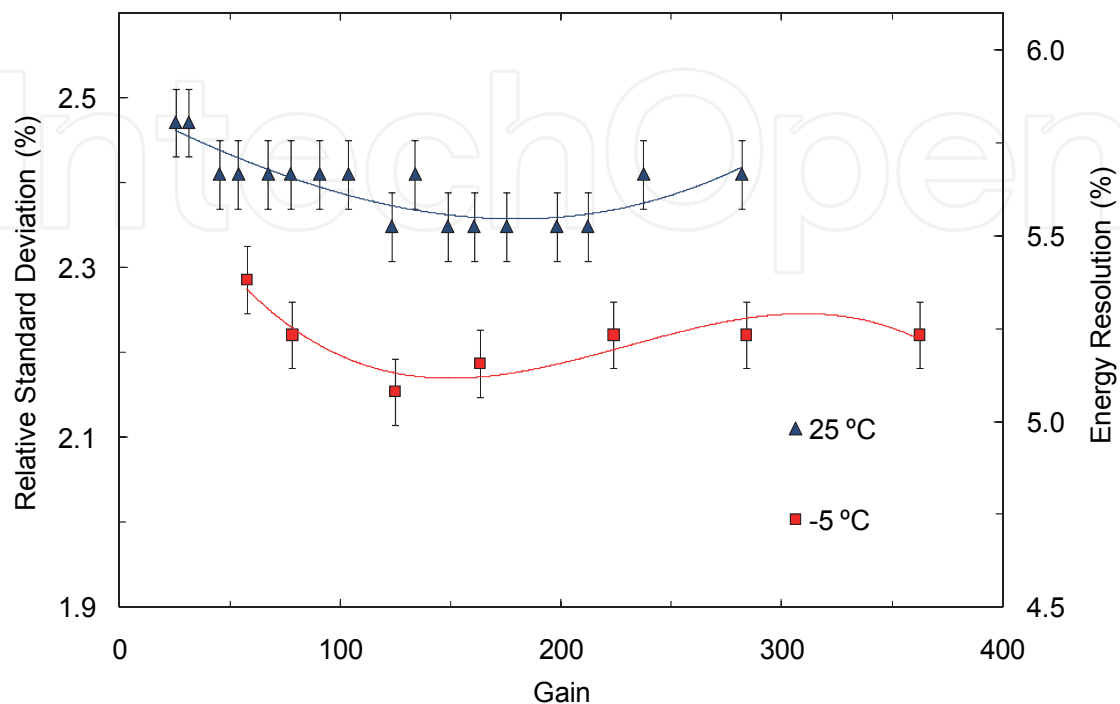
Fig. 15. Relative statistical fluctuations associated to the detection of 2.7×10^4 VUV photons of ~172 nm light pulses as a function of APD gain for operation temperatures of 25°C and -5°C. The lines serve only to guide the eyes.

8. Behaviour under intense magnetic fields

The insensitivity of the APD response to magnetic fields in X-ray and visible-light detection is well documented [23, 25, 42]. In opposition to visible light and X-ray detection, where the APD response is insensitive to magnetic fields, VUV detection with APDs is sensitive to magnetic fields. Figure 16 presents the pulse-height distribution obtained for VUV xenon-scintillation pulses for magnetic fields of 0 and 5 T, at room temperature. As can be seen, there is a significant reduction in the APD gain at high magnetic fields.

Figure 17 shows the APD relative pulse amplitude and energy resolution as a function of magnetic field for the xenon scintillation peak. As shown, for VUV-light the relative amplitude decreases gradually as the magnetic field is applied, reaching a 24% reduction at 5 T. The energy resolution increases from 13% to 15%. Since VUV photons interact within the first few atomic layers of silicon, where the electric field is weak, the magnetic field influences drift and diffusion of the produced photoelectrons, leading to partial charge loss to the dead layer at the APD entrance.
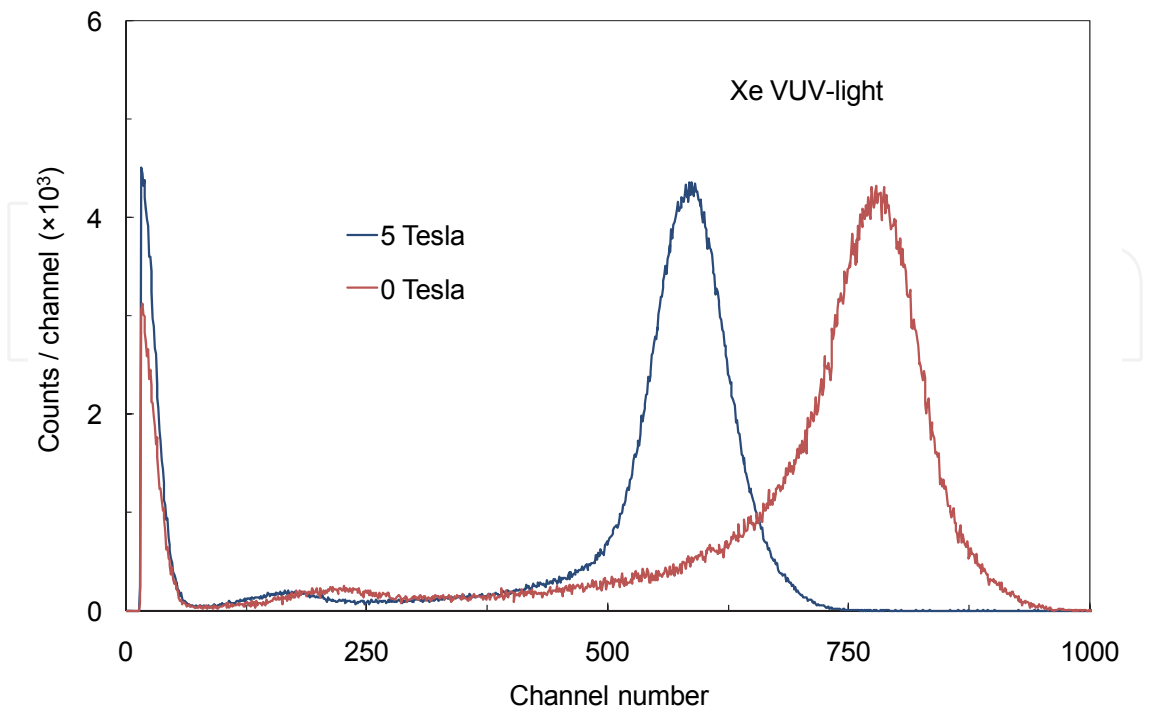
Fig. 16. APD pulse-height distributions for xenon scintillation light resulting from 5.9-keV X-rays absorbed in a xenon GPSC operating under magnetic field intensities of 0 T and 5 T.
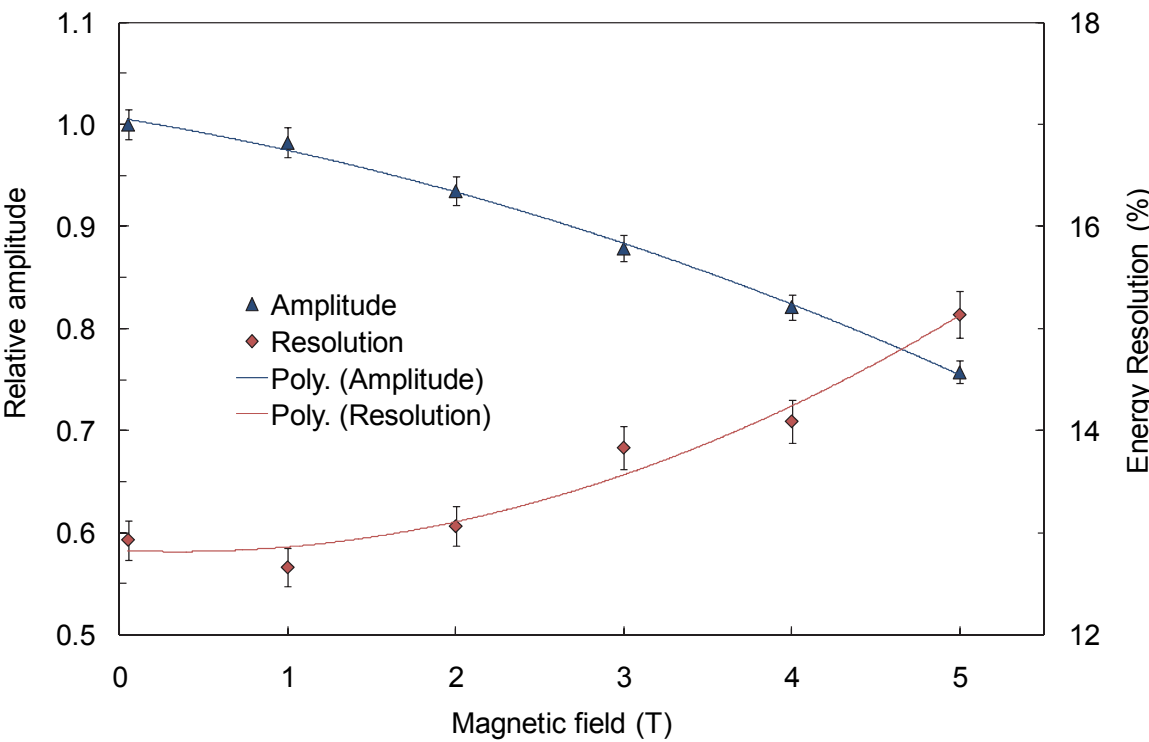

Fig. 17. Relative pulse amplitude and energy resolution as a function of magnetic field intensity for xenon VUV scintillation detection.

9. Conclusions

The APD is a suitable device for the detection of VUV light pulses of photons down to about 120 nm. PMTs present a sensitivity range down to 115 nm- with MgF_2 windows -, gains above 10^7, dark currents below a few nA instead of a few hundred nA for APDs, and are suitable for single photon detection. However, the photodiode compactness, reduced power consumption, simple operation and straightforward photon calibration are significant advantages over PMTs.

Figures 6 and 9 present the results for the Minimum number of Detectable Photons (MDP), defined as the number of VUV photons that would produce a signal in the APD with an amplitude equivalent to the onset of the electronic noise tail. The minimum number of photons that can be detected with the APD, for this experimental setup, are about 1300 and 600 for 128- and 172 nm, respectively, almost three orders of magnitude higher than is the case for PMTs. Therefore, the APD is not suitable for single photon detection and VUV-photon spectrometry. Nevertheless, it can be applied to synchrotron radiation in VUV-photon detection and to other areas of optics, where the light levels are adequate for its use.

The MDP for 172-nm photons is about half of that for 128 nm photons, achieving the lowest values for lower gains. This difference reflects the higher spectral sensitivity of these APDs for 172 nm, which is approximately 150 mA/W, corresponding to an average number of 1.1 free electrons produced in the APD per incident VUV-photon, when compared to 50 mA/W that corresponds to an average number of 0.55 free electrons produced in the photodiode per incident VUV-photon for 128 nm [19]. In fact, it is the number of primary charge carriers that defines the corresponding signal amplitude and the signal-to-noise ratio.

Figures 7 and 10 depict also the results of the relative statistical fluctuations associated to the VUV detection of 2.4×10^4 photons of 172-nm VUV-light pulses and 1.4×10^4 photons of 128-nm, respectively. These values are 3.9% and 2.2%, respectively. This difference is consistent with the dependence of the APD resolution on the inverse of the square root of the number of the charge carries produced in the photodiode [30] and it reflects not only the difference in the number of photons involved in each case, but also the difference in the respective quantum efficiency. The numbers of charge carriers produced in the APD are

$2.4 \times 10^4 \times 1.1 = 2.64 \times 10^4$ free electrons for xenon

and

$1.4 \times 10^4 \times 0.55 = 7.7 \times 10^3$ free electrons for argon,

being

$$2.2 \times \sqrt{\frac{26400}{7700}} \cong 3.9 \ .$$

This is also consistent with the results for visible (red) light from a LED obtained in [22], with an energy resolution of 7% for 2600 free electrons produced in the APD.

For the present charge carrier quantities, APD gains as low as 30 to 60 are enough to obtain best performances. However, gains as low as 20 and 30, respectively, are sufficient to achieve a nearly optimum performance, i.e. without presenting significant degradation of MDP and energy resolution. For lower light levels, higher gains will be needed to pull the signal of the light-pulse out of the noise and achieve the best possible performance.

The experimental results presented in this chapter show that both MDP and statistical fluctuations associated to light detection do not depend on photon wavelength, but rather

on the number of charge carriers produced by the light-pulse in the APD. This is at odds with other effects like light-to-X-rays non-linearity and amplitude behaviour under intense magnetic fields, where the photon interaction in the first atomic layers of the wafer has a significant influence on these results.

In addition to space charge effects resulting from the point-like nature of X-ray interactions, our results suggest a dependence of the non-linearity on the light wavelength. The X-ray to light gain non-linearity for 128 nm VUV photons is higher than the one obtained for 172 nm VUV photons and both are higher than that reported for visible light [30]. The non-linearity must depend on the penetration depth in silicon of each type of light. For both VUV and visible light, photons are absorbed in the drift region of the APD, where the electric field is weak and the effect of capture of charges is more significant. Since the absorption is much more superficial for VUV light (~5 nm), capture is greater in this case but decreases with gain due to the electric field increase. Thus, the higher APD voltage results in a more efficient collection of the primary electrons produced near the entrance surface for argon, whereas this effect is smaller for xenon and most probably negligible for visible light since the penetration depth increases. The shallow penetration of the VUV photons may also explain the different behaviour of the APD response under intense magnetic fields for VUV and visible light detection.

10. Acknowledgements

11. References

[1] Windowless Series large area APD, Advanced Photonics Inc., 1240 Avenida Acaso Camarillo, CA 93012, USA.

[2] VUV-sensitive large area APD, Radiation Monitoring Devices, Inc., 44 Hunt Street, Watertown, MA 02472, USA.

[3] S-8664-55-SPL large area APD, Hamamatsu Photonics K.K., 325-6, Sunayama-cho, Naka-ku, Hamamatsu City, Shizuoka Pref., 430-8587, Japan.

[4] J.A.M. Lopes, J.M.F. dos Santos, R.E. Morgado, C.A.N. Conde, "A xenon gas proportional scintillation counter with a UV-sensitive large-area avalanche photodiode", IEEE Trans. Nucl. Sci. 48 (2001) 312-319.

[5] C.M.B. Monteiro, J.A.M. Lopes, P.C.P.S. Simões, J.M.F. dos Santos, C.A.N. Conde, "An argon gas proportional scintillation counter with UV avalanche photodiode scintillation readout", IEEE Trans. Nucl. Sci. 48 (2001) 1081-1086.

[6] R. Neilson, _, F.LePort, A.Pocar, K.S.Kumar, A.Odian et al., "Characterization of large area APDs for the EXO-200 detector", Nucl. Instrum. Meth. A 608 (2009) 68–75.

[7] V.N. Solovov, V. Chepel, M.I. Lopes, R. Ferreira Marques and A.J.P.L. Policarpo, "Study of large area avalanche photodiodes for detecting liquid xenon scintillation", IEEE Trans. Nucl. Sci. 47 (2000) 1307-1310.

[8] V.N. Solovov, A. Hitachi, V. Chepel, M.I. Lopes, R. Ferreira Marques, A.J.P.L. Policarpo, "Detection of scintillation light of liquid xenon with a LAAPD", Nucl. Instr. Meth. A 488 (2002) 572-578.

[9] K. Ni, E. Aprile, D. Day, K.L. Giboni, J.A.M. Lopes, P. Majewski and M. Yamashita "Performance of a large area avalanche photodiode in a liquid xenon ionization and scintillation chamber", Nucl. Instrum. Meth. A 551 (2005) 356.

[10] P. Shagin, R. Gomez, U. Oberlack, P. Cushman, B. Sherwood, M. McClish and R. Farrell, "Avalanche Photodiode for liquid xenon scintillation: Quantum Efficiency and gain", J. Inst. 4 (2009)P01005.

[11] J. C. Campbell, S. Demiguel, F. Ma, A. Beck, X. Guo, S. Wang, X. Zheng, X. Li, J. D. Beck, M. A. Kinch, A. Huntington, L. A. Coldren, J. Decobert, and N. Tscherptner, "Recent Advances in Avalanche Photodiodes," IEEE J. of Sel. Topics in Quantum Electronics 10 (2004) 777.

[12] Q. Wang, S. Savage, B. Noharet, I. Petermann, S. Persson, S. Almqvist, M. Bakowski, J.Y. Andersson, "Analysis and comparison of UV photodetectors based on wide bandgap semiconductors", Proceedings of SPIE-The International Society for Optical Engineering, Vol. 7602 (2010).

[13] R. McClintock, E. Cicek, Z. Vashaei, C. Bayram, M. Razeghi, M.P. Ulmer, "III-Nitride Based Avalanche Photo Detectors", Proceedings of SPIE-The International Society for Optical Engineering, Vol. 7780 (2010).

[14] E. Cicek, Z. Vashaei, C. Bayram, R. McClintock, M. Razeghi, M.P. Ulmer, "Comparison of ultraviolet APDs grown on free-standing GaN and sapphire substrates", Proceedings of SPIE-The International Society for Optical Engineering, Vol. 7780 (2010).

[15] S.M. Savage, A. Schoner, I. Petermann, M. Bakowski, "Sensitive and stable SiC APD for UV detection", Proceedings of SPIE-The International Society for Optical Engineering, Vol. 7726 (2010).

[16] G.A. Shaw, A.M. Siegel, J. Model, A. Geboff, S. Soloviev, A. Vert, P. Sandvik, "Deep UV Photon-Counting Detectors and Applications", Proceedings of SPIE-The International Society for Optical Engineering, Vol. 7320 (2009).

[17] S. Soloviev, A. Vert, A. Bolotnikov, P. Sandvik, "UV SiC avalanche photodetectors for photon counting", IEEE SENSORS, VOLS 1-3 (2009) 1819.

[18] T. Takahashi, S. Himi, M. Suzuki, J. Ruan, S. Kubota, "Emission spectra from Ar-Xe, Ar-Kr, Ar-N2, Ar-CH4, Ar-CO2 and Xe-N2 gas scintillation proportional counters", Nucl. Instr. Meth. A 205 (1983) 591-596.

[19] Advanced Photonix Inc. Application Notes: "Windowless large area APDs" (1999).

[20] L.M.P. Fernandes, J.A.M. Lopes, C.M.B. Monteiro, J.M.F. dos Santos, R.E. Morgado, "Non-linear behaviour of large-area avalanche photodiodes", Nucl. Instr. Meth. A 478 (2002) 395-399.

[21] J.A.M. Lopes, L.M.P. Fernandes, J.M.F. dos Santos, R.E. Morgado, C.A.N. Conde, "VUV detection in large-area avalanche photodiodes as a function of temperature", Nucl. Instr. Meth. A 504 (2003) 331-334.

[22] L.M.P. Fernandes, J.A.M. Lopes, J.M.F. dos Santos, P.E. Knowles, F. Mulhauser, L. Ludhova, F. Kottmann, R. Pohl, D. Taqqu, "LAAPD low temperature performance in x-ray and visible-light detection", IEEE Trans. Nucl. Sci. 51 (2004) 1575-1580.

[23] L.M.P. Fernandes, A. Antognini, M. Boucher, C.A.N. Conde, O. Huot, P.E. Knowles, F. Kottmann, L. Ludhova, F. Mulhauser, R. Pohl, L.A. Schaller, J.M.F. dos Santos, D. Taqqu, J.F.C.A. Veloso, "Behaviour of large-area avalanche photodiodes under intense magnetic fields for VUV, visible and X-ray photon detection", Nucl. Instr. Meth. A 498 (2003) 362-368.

[24] C.M.B. Monteiro, L.M.P. Fernandes, J.A.M. Lopes, J.F.C.A. Veloso, J.M.F. dos Santos, "Detection of VUV photons with large-area avalanche photodiodes", Appl. Phys. B 81 (2005) 531-535.

[25] A.Q.R. Baron and S.L. Ruby, "Time resolved detection of X-rays using large area avalanche photodiodes", Nucl. Instr. Meth. A 343 (1994) 517.

[26] E.M. Gullikson, E. Gramsch, M. Szawlowski, "Large-area avalanche photodiodes for the detection of soft X-rays", Appl. Optics 34 (1995) 4662.

[27] Pansart J P, Avalanche photodiodes for particle detection, Nucl. Instr. Meth. A 387 (1997) 186.

[28] M. Moszynski, M. Kapusta, M. Balcerzyk, M. Szawlowski, D. Wolski, I. Wegrzecka, M. Wegrzecki, "Comparative study of avalanche photodiodes with different structures in scintillation detection", IEEE Trans. Nucl. Sci. 48 (2001) 1205-1210.

[29] T.W. Barnard, M.I. Crockett, J.C. Ivaldi, P.L. Lundberg, D.A. Yates, P.A. Levine, D.J. Sauer, "Solid-state detector for ICP-OES", Anal. Chem. 65 (1993) 1231-1239.

[30] M. Moszynski, M. Szawlowski, M. Kapusta, M. Balcerzyk, "Large area avalanche photodiodes in scintillation and X-rays detection", Nucl. Instr. Meth. A 485 (2002) 504.

[31] R.J. McIntyre, "The distribution of gains in uniformly multiplying avalanche photodiodes: theory", IEEE Trans. Electron Devices 19 (1972) 703.

[32] L.M.P. Fernandes, J.A.M Lopes, J.M.F dos Santos, "Excess noise factor in large area avalanche photodiodes for different temperatures", Nucl. Instr. Meth. A 531 (2004) 566.

[33] P.W. Nicholson, *Nuclear Electronics*, Wiley-Interscience Publication (1974), John Wiley & Sons, London.

[34] R.J. McIntyre, "Multiplication noise in uniform avalanche diodes", IEEE Trans. Electron Devices 13 (1966) 164.

[35] P.P. Webb, R.J. McIntyre, "Large area reach-through avalanche diodes for X-ray spectroscopy", IEEE Trans. Nucl. Sci. 23 (1976) 138.

[36] J.M.F. dos Santos, J.A.M. Lopes, J.F.C.A. Veloso, P.C.P.S. Simões, T.H.V.T. Dias, F.P. Santos, P.J.B.M. Rachinhas, L.F.R. Ferreira, C.A.N. Conde, "Development of portable gas proportional scintillation counters for X-ray spectrometry", X-Ray Spectrom. 30 (2001) 373.

[37] C.M.B. Monteiro, L.M.P. Fernandes, J.A.M. Lopes, L.C.C. Coelho, J.F.C.A. Veloso, J.M.F. dos Santos, K. Giboni, E. Aprile, "Secondary scintillation yield in pure xenon", J. Inst. 2 (2007) P05001.

[38] C.M.B. Monteiro, J.F.C.A. Veloso, J.A.M. Lopes, J.M.F. dos Santos, "Secondary scintillation yield in pure argon", Phys. Lett. B 668 (2008) 167.

[39] C. M. B. Monteiro, A. S. Conceição, F. D. Amaro, J. M. Maia, A. C. S. S. M. Bento et al., "Secondary scintillation yield from gaseous micropattern electron multipliers in direct Dark Matter detection", Physics Letters B 677 (2009) 133.

[40] E.D.C. Freitas, C.M.B. Monteiro, M. Ball, J. J. Gómez-Cadenas, J.A.M. Lopes,, T. Lux, F. Sánchez, J.M.F. dos Santos, "Secondary Scintillation Yield in High-Pressure Xenon Gas for neutrinoless double beta decay search", Physics Letters B 684 (2010) 205.

[41] L.M.P. Fernandes, F.D. Amaro, A. Antognini, J.M.R. Cardoso, C.A.N. Conde, O. Huot, P.E. Knowles, F. Kottmann, J.A.M. Lopes, L. Ludhova, C.M.B. Monteiro, F. Mulhauser, R. Pohl, J.M.F. dos Santos, L.A. Schaller, D. Taqqu, J.F.C.A. Veloso, "Characterization of large area avalanche photodiodes in X-ray and VUV-light detection", J. Inst. 2 (2007) P08005.

[42] A. Karar, Y. Musienko, J. Ch. Vanel, "Characterization of avalanche photodiodes for calorimetry applications", Nucl. Instr. Meth. A 428 (1999) 413-431.
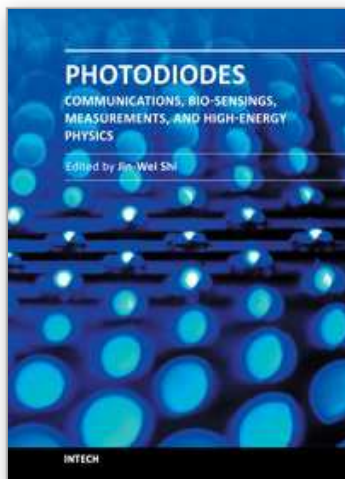
Photodiodes - Communications, Bio-Sensings, Measurements and High-Energy Physics

Edited by Associate Professor Jin-Wei Shi

This book describes different kinds of photodiodes for applications in high-speed data communication, biomedical sensing, high-speed measurement, UV-light detection, and high energy physics. The photodiodes discussed are composed of several different semiconductor materials, such as InP, SiC, and Si, which cover an extremely wide optical wavelength regime ranging from infrared light to X-ray, making the suitable for diversified applications. Several interesting and unique topics were discussed including: the operation of high-speed photodiodes at low-temperature for super-conducting electronics, photodiodes for bio-medical imaging, single photon detection, photodiodes for the applications in nuclear physics, and for UV-light detection.

How to reference

In order to correctly reference this scholarly work, feel free to copy and paste the following:

INTECH
open science | open minds